TM-70-1011-7

TECHNICAL MEMORANDUM

COMPUTATION OF THREE-DIMENSIONAL SUPERSONIC FLOWS WITH SHOCK WAVES

Bellcomm

BELLCOMM, INC.
955 L'ENFANT PLAZA NORTH, S.W. WASHINGTON, D.C. 20024

COVER SHEET FOR TECHNICAL MEMORANDUM

TITLE- Computation of Three-Dimensional Supersonic Flows with Shock Waves

TM- 70-1011-7

DATE- August 6, 1970

FILING CASE NO(S)- 103-7

AUTHOR(S)- I.O. Bohachevsky

FILING SUBJECT(S)- Reentry Phenomena
(ASSIGNED BY AUTHOR(S)- Supersonic Flow

ABSTRACT

This memorandum describes a simple numerical method for the computation of three-dimensional supersonic flows. The simplicity of the approach results from the use of a finite difference scheme that does not require a shock fitting procedure but permits a direct integration of the equations of motion in the axial direction. Application to non-symmetric (at an angle of attack) conical flows is presented and compared with other solutions of the same problem and with experimental data. The idiosyncrasies of the technique are discussed and a direction for further development of this approach is indicated.

BELLCOMM, INC.
955 L'ENFANT PLAZA NORTH, S.W. WASHINGTON, D.C. 20024

SUBJECT: Computation of Three-Dimensional Supersonic Flows with Shock Waves

DATE: August 6, 1970

FROM: I. O. Bohachevsky

TM-70-1011-7

TECHNICAL MEMORANDUM

I. PREFACE

The purpose of this memorandum is to introduce the topic of the numerical determination of supersonic flows surrounding bodies of revolution employed for purposes of atmospheric entry and to describe the general ideas involved in this problem.

This aim will be accomplished by first briefly describing and characterizing the existing methods for the computation of the above specified flow fields, then introducing an exploratory approximate technique for this purpose, obtaining solutions with it and comparing them with experimental results, and finally discussing the properties and limitations of the novel approach employed here. This discussion will serve as a motivation for the numerical investigations proposed and currently pursued at Bellcomm.(1)

The computations described in the present memorandum constitute a natural extension of the work on the determination of the flow-field for an Apollo shaped body reported by Bohachevsky and collaborators in References (2) and (3). They were performed by the author under NASA sponsorship prior to joining the staff of Bellcomm but have not been reported previously.

II. INTRODUCTION

Because of ease of manufacture and many other considerations, bodies of revolution are very popular in application to spacecraft designed to enter planetary atmospheres. The knowledge of the flow field surrounding these bodies during the atmospheric entry is important for many reasons. For example, pressure distribution in the inviscid flow is necessary for the calculation of the aerodynamic forces and together with the velocity distribution is required in the boundary layer computations from which skin friction and heat transfer are obtained.

For conical bodies with cone angles that are less than a critical value (depending on the Mach number), the shock wave which forms during high velocity entry into the atmosphere is attached and the flow behind it remains supersonic. This is the case also in the afterbody region of slender reentry shapes. The problem of the determination of such supersonic flow fields has received considerable attention for many years. There exist presently numerous methods for their computation, all of which, however, are different variations of these basic three types:

1. the celebrated method of characteristics,[4][5]
2. the double sweep method,[6][7] similar to the technique commonly used in boundary layer computations, and
3. the method of strips or integral relations.[8][9]

All of the above approaches make essential use of coordinate systems that depend on the unknown solution; this property makes the computational procedure awkward and requires integration of additional equations to locate the coordinate system in the physical space. Under certain conditions, however, other considerations may outweigh these disadvantages.

For example: The tracing of characteristics greatly increases the accuracy and speed of computation when there exist quantities which remain constant along them, i.e., Riemann Invariants. This is the case in isentropic, steady two-dimensional or unsteady one-dimensional flows; the present interest, however, lies in three-dimensional radiating and/or reacting flows. A simple computation, described in the Appendix, establishes the fact that outside of the above-mentioned two cases the Riemann Invariants do not exist. The determination of characteristics then becomes a liability instead of an asset.

The double sweep method has been used successfully and effectively, however, it is cumbersome and requires, like the method of characteristics, a shock fitting procedure which implies iterations.

The method of integral relations is of limited accuracy and requires intricate programming to handle the singular sonic points; the labor required for its application increases much more rapidly than accuracy when better than one (or two) strip approximations are desired.

We felt, therefore, that there was need for a conceptually simple technique to determine the flow field that would enable design engineers to use computers without extensive knowledge of numerical analysis or intricate programming techniques. Such a method becomes possible when the cumbersome shock fitting procedure is eliminated. This is achieved by employing a finite difference scheme with the following two properties:

1. retention of validity across discontinuities, and
2. ability to automatically satisfy Rankine-Hugoniot conditions where shocks form.

These requirements were formulated in Refs. (2) and (3); included there is also a discussion of the simplifications in the computational procedure possible because of them and of the price in precision and resolution that must be paid for these simplifications. It was found that the results are acceptable for many purposes. A possible way to improve the accuracy will be indicated in the last section of this memorandum.

Of the several schemes that possess the above two properties and are available for our purposes[(2)] a generalization of Lax's scheme is chosen because of its simplicity, as was done in References (2) and (3). The present application, therefore, is a natural extension of the work reported previously[(2)(3)] to steady flow fields; the possibility of such extension has been pointed out in Reference (2).

It may appear strange at first, but the computation of steady flow fields is more involved than the previous work on the unsteady flows. The reason is purely algebraic; it will become clear from the form of the governing equations, given in Section III, that to recover the flow variables from the steady state form of the conservation variables now is no longer as trivial an operation as it was in the unsteady case. The recovery in the present case requires additional complex algebraic operations.

The memorandum is organized as follows: in Section III, we formulate the differential problem and in Section IV we describe the finite difference procedure, the associated boundary logic, and the required initial conditions. The presentation and discussion of results in Section V lead to an alternate but more restrictive formulation and solution of the problem in Section VI. The memorandum is concluded with a general discussion contained in Section VII.

III. FORMULATION OF THE PROBLEM

For the description of the flow field in the vicinity of a body of revolution cylindrical coordinates with the z-axis aligned along the body axis are most convenient. Figure 1 illustrates the coordinate system used in this paper and the general field configuration. The problem is: to determine the distribution of flow variables in all downstream planes $z > z_o$ from the knowledge of them in a given plane $z = z_o$.

The initial distribution at $z = z_o$ may be obtained by the present method when the shape is pointed and the shock wave attached, otherwise it must be determined by some other method. Sections V and VI of this memorandum comment on this phase of the problem in more detail.

In cylindrical coordinates, the conservation form of the governing differential equations is:

$$\frac{\partial}{\partial z}(\rho w) = -\frac{\partial}{\partial r}(\rho u) - \frac{1}{r}\frac{\partial}{\partial \phi}(\rho v) - \frac{1}{r}(\rho u) \tag{1}$$

$$\frac{\partial}{\partial z}(\rho w u) = -\frac{\partial}{\partial r}(\rho u^2 + p) - \frac{1}{r}\frac{\partial}{\partial \phi}(\rho u v) + \frac{\rho}{r}(v^2 - u^2) \tag{2}$$

$$\frac{\partial}{\partial z}(\rho w v) = -\frac{\partial}{\partial r}(\rho u v) - \frac{1}{r}\frac{\partial}{\partial \phi}(\rho v^2 + p) - \frac{2}{r}(\rho u v) \tag{3}$$

$$\frac{\partial}{\partial z}(\rho w^2 + p) = -\frac{\partial}{\partial r}(\rho u w) - \frac{1}{r}\frac{\partial}{\partial \phi}(\rho v w) - \frac{\rho}{r}(u w) \tag{4}$$

$$\frac{\partial}{\partial z}\left[\rho w\left(\frac{1}{2}q^2 + h\right)\right] = -\frac{\partial}{\partial r}\left[\rho u\left(\frac{1}{2}q^2 + h\right)\right] - \frac{1}{r}\frac{\partial}{\partial \phi}\left[\rho v\left(\frac{1}{2}q^2 + h\right)\right]$$

$$- \frac{1}{r}\left[\rho u\left(\frac{1}{2}q^2 + h\right)\right] \tag{5}$$

where r, ϕ, and z are the coordinates as indicated in Figure 1, u, v, and w are the corresponding velocity components, ρ is the density, p is the pressure, h is the enthalpy per unit mass, and $q^2 = u^2 + v^2 + w^2$.

To form a closed system Equations (1) to (5) must be supplemented with a thermodynamic relation $h = h(\rho, p)$; for an ideal gas this relation may be expressed in the form:

$$h = \frac{\gamma}{\gamma-1} \frac{p}{\rho} \tag{6}$$

where γ is the constant ratio of specific heats.

The solution of Equations (1)-(6) is sought in an open-ended domain bounded by $z = z_o$ and $r = R(z)$ which specifies the body surface. At $r = R$, we should prescribe only the vanishing of the normal velocity component; for the description of separated or wake flows this condition must be replaced by a constant-pressure free-boundary condition.

In addition, the solution should tend to the free stream as $r \to \infty$ or it should actually assume free stream values outside of the region bounded by the shock wave.

IV. THE INTEGRATION PROCEDURE

The desired solution will be obtained by numerical integration. Towards this end, Equations (1) to (5) are represented by their finite difference analogues with the radial and azimuthal derivatives replaced by central differences and the axial derivative replaced by a forward difference where, in the place of the starting value, the average value of its four neighbors is used. Thus, with the superscript n denoting the axial (z) position, and subscripts ℓ and k the radial (r) and azimuthal (ϕ) positions in the mesh, the finite difference form of Equations (1) to (5) is:

$$\left(\rho w\right)_{\ell,k}^{n+1} = \frac{1}{4}\left[\left(\rho w\right)_{\ell+1,k}^{n} + \left(\rho w\right)_{\ell-1,k}^{n} + \left(\rho w\right)_{\ell,k+1}^{n} + \left(\rho w\right)_{\ell,k-1}^{n}\right]$$

$$- \frac{\Delta z}{2\Delta r}\left[\left(\rho u\right)_{\ell+1,k}^{n} - \left(\rho u\right)_{\ell-1,k}^{n}\right] \qquad (7)$$

$$- \frac{1}{r_\ell}\frac{\Delta z}{2\Delta\phi}\left[\left(\rho v\right)_{\ell,k+1}^{n} - \left(\rho v\right)_{\ell,k-1}^{n}\right]$$

$$- \frac{\Delta z}{r_\ell}\left(\rho u\right)_{\ell,k}^{n}$$

$$\left(\rho wu\right)_{\ell,k}^{n+1} = \frac{1}{4}\left[\left(\rho wu\right)_{\ell+1,k}^{n} + \left(\rho wu\right)_{\ell-1,k}^{n} + \left(\rho wu\right)_{\ell,k+1}^{n} + \left(\rho wu\right)_{\ell,k-1}^{n}\right]$$

$$- \frac{\Delta z}{2\Delta r}\left[\left(\rho u^2 + p\right)_{\ell+1,k}^{n} - \left(\rho u^2 + p\right)_{\ell-1,k}^{n}\right] \qquad (8)$$

$$- \frac{\Delta z}{r_\ell 2\Delta\phi}\left[\left(\rho uv\right)_{\ell,k+1}^{n} - \left(\rho uv\right)_{\ell,k-1}^{n}\right]$$

$$+ \frac{\Delta z}{r_\ell}\left[\rho\left(v^2 - u^2\right)\right]_{\ell,k}^{n}$$

$$\left(\rho wv\right)^{n+1}_{\ell,k} = \frac{1}{4}\left[\left(\rho wv\right)^{n}_{\ell+1,k} + \left(\rho wv\right)^{n}_{\ell-1,k} + \left(\rho wv\right)^{n}_{\ell,k+1} + \left(\rho wv\right)^{n}_{\ell,k-1}\right]$$

$$- \frac{\Delta z}{2\Delta r}\left[\left(\rho uv\right)^{n}_{\ell+1,k} - \left(\rho uv\right)^{n}_{\ell-1,k}\right]$$

$$- \frac{\Delta z}{r_{\ell}2\Delta\phi}\left[\left(\rho v^{2} + p\right)^{n}_{\ell,k+1} - \left(\rho v^{2} + p\right)^{n}_{\ell,k-1}\right] \tag{9}$$

$$- \frac{2\Delta z}{r_{\ell}}\left(\rho uv\right)^{n}_{\ell,k}$$

$$\left(\rho w^{2} + p\right)^{n+1}_{\ell,k} = \frac{1}{4}\left[\left(\rho w^{2} + p\right)^{n}_{\ell+1,k} + \left(\rho w^{2} + p\right)^{n}_{\ell-1,k} + \right.$$

$$\left. + \left(\rho w^{2} + p\right)^{n}_{\ell,k+1} + \left(\rho w^{2} + p\right)^{n}_{\ell,k-1}\right]$$

$$- \frac{\Delta z}{2\Delta r}\left[\left(\rho uw\right)^{n}_{\ell+1,k} - \left(\rho uw\right)^{n}_{\ell-1,k}\right] \tag{10}$$

$$- \frac{\Delta z}{r_{\ell}2\Delta\phi}\left[\left(\rho vw\right)^{n}_{\ell,k+1} - \left(\rho vw\right)^{n}_{\ell,k-1}\right]$$

$$- \frac{\Delta z}{r_{\ell}}\left(\rho uw\right)^{n}_{\ell,k}$$

$$\left[\rho w\left(\frac{1}{2} q^2 + h\right)\right]^{n+1}_{\ell,k} = \frac{1}{4}\left\{\left[\rho w\left(\frac{1}{2} q^2 + h\right)\right]^{n}_{\ell+1,k} + \left[\rho w\left(\frac{1}{2} q^2 + h\right)\right]^{n}_{\ell-1,k}\right.$$

$$\left. + \left[\rho w\left(\frac{1}{2} q^2 + h\right)\right]^{n}_{\ell,k+1} + \left[\rho w\left(\frac{1}{2} q^2 + h\right)\right]^{n}_{\ell,k-1}\right\}$$

$$- \frac{\Delta z}{2\Delta r}\left\{\left[\rho u\left(\frac{1}{2} q^2 + h\right)\right]^{n}_{\ell+1,k} - \left[\rho u\left(\frac{1}{2} q^2 + h\right)\right]^{n}_{\ell-1,k}\right\} \qquad (11)$$

$$- \frac{\Delta z}{r_\ell 2\Delta\phi}\left\{\left[\rho v\left(\frac{1}{2} q^2 + h\right)\right]^{n}_{\ell,k+1} - \left[\rho v\left(\frac{1}{2} q^2 + h\right)\right]^{n}_{\ell,k-1}\right\}$$

$$- \frac{\Delta z}{r_\ell}\left[\rho u\left(\frac{1}{2} q^2 + h\right)\right]^{n}_{\ell,k}$$

For the purpose of this paragraph only we omit the indices and denote the right hand sides of Equations (7) through (11) by A, B, C, D, and E. Then, after integrating Equations (7) to (11) one step in the z direction, we obtain a system of algebraic recovery equations:

$$\rho w = A \qquad (12)$$

$$\rho w u = B \qquad (13)$$

$$\rho w v = C \qquad (14)$$

$$(\rho w^2 + p) = D \qquad (15)$$

$$\rho w\left(\frac{1}{2} q^2 + h\right) = E \qquad (16)$$

from which ρ, u, v, w, and p are to be determined.

Equations (12) to (16), in general, must be solved by iterations; it is this fact that, as noted in the Introduction, makes the present steady state computations more complex than the previous unsteady ones[2],[3]. In the case of an ideal gas, however, when Equation (6) is valid, the above system can easily be reduced to a single quadratic equation for p from which the solution with the negative square root must be chosen.

Equations (6) to (16), therefore, completely describe the numerical algorithm for the determination of the values of flow variables at $z = (n+1)\Delta z$ from those at $z = n\Delta z$. The computations can now be carried as far downstream as desired.

The boundary conditions are numerically satisfied in the following manner: the upper end of the mesh is chosen outside of the shock envelope and after each step in the z direction, all flow variables at an auxiliary point $r_{max} + \Delta r$ are set equal to their free stream values.

On the surface of the body, $r = R(z)$, the boundary logic is considerably more involved because the body is not one of the coordinate surfaces. A fictitious point is located inside the body and to it are assigned the values of p, ρ and q equal to the values of these quantities at the first mesh point outside of the body. The flow direction, however, is assigned in such a way that, when a linear interpolation is performed between these two points, the streamline direction will equal the slope of the body surface at the point where it intersects the radial line joining the mesh points inside and outside of the body. When the mesh point is less than, say, $.05\Delta r$ away from R then it is assumed to lie on the body surface and the velocity is adjusted accordingly.

Several other, algebraically equivalent, ways to enforce the tangency of the flow were tried. Some of them can be made more accurate; some, however, may render the overall computation process unstable. Thus, different choices of boundary logic should be tested primarily for stability properties.

The stability of the finite difference scheme described thus far may be estimated using the linear Courant-Friedrichs-Lewy condition[2] which requires that the end of each z step should not be outside of the Mach cone passing through meshpoints adjacent to the point at which the computation is being performed. Translation of this requirement into algebraic language yields:

$$\frac{\Delta z}{\Delta r} \leq \frac{w^2 - a^2}{|uw| + a\sqrt{u^2+w^2-a^2}} \tag{17}$$

$$\frac{\Delta z}{(R+\ell\Delta r)\Delta\theta} \leq \frac{w^2-a^2}{|vw| + a\sqrt{v^2+w^2-a^2}} \tag{18}$$

where a is the speed of sound.

A special feature of the problem being considered is the fact that the shock position can be forecast fairly accurately. Therefore the maximum value of $R + \ell\Delta r$ can be predicted in advance which makes inequality (18) useful.

Both inequalities (17) and (18) should be satisfied in the flow field locally. This can be achieved in either of two ways:

1. Estimate a priori the smallest value that the right hand sides will assume anywhere in the field and use a compatible fixed mesh.

2. Before each computational step search for the minimum of both right hand sides and use the appropriate step in the z direction. It is doubtful, however, whether the saving in computing time from using the maximum allowable Δz at each step will compensate for the time lost in search of the required minima.

For the best definition of the shock the ratio $\frac{\Delta z}{\Delta r}$ should be as large as (17) or (18) or other, empirically derived, stability condition allows.(2)(3)

If the nose section of the body is such that the shock wave remains attached (which will be the case in examples presented here), then the present formulation can be used throughout the entire field by locating the initial plane $z = z_o$ at the sharp apex. The computation is not performed at the very vertex, $R = 0$; instead we set there $u = w \operatorname{tg} \beta$ (β is the cone half angle) and all other variables equal to their free stream values.

If the bow shock wave is detached then the method of Reference 3 or an equivalent treatment of the so called "blunt body problem" must be employed to obtain the initial conditions necessary to begin present computations.

V. PRESENTATION AND DISCUSSION OF NUMERICAL RESULTS

In the present section we illustrate and discuss the procedure by presenting results of the numerical determination of the flow about a sharp cone, with cone half angle $\beta=15°$, oriented at an angle of attack $\alpha=10°$ to a free stream of air characterized by the Mach number $M_o=7$.

Steady flows over sharp cones exhibit conical similarity when the shock waves are attached, therefore the presence of such property in our solution would be a qualitative indication of the validity of the present approach. To verify this property Figure 2 was prepared; it represents the surface density distribution as a function of the axial distance from the vertex on the windward ($\phi=90°$) and leeward ($\phi=-90°$) sides of the cone. From this result we see that, although the computation may be started at the vertex without difficulty, it requires about 300 axial steps to attain the correct value.

The waviness of the curves in Figure 2 is caused by the nonuniformness of the boundary conditions: when the cone surface periodically approaches close to, or coincides with, a meshpoint, boundary logic different from interpolation results in a small perturbation.

Figures 3 and 4 represent density distributions along the normal to the cone axis (across the shock layer) and on the cone surface around the circumference at $z = 219\Delta z$ obtained from the calculational procedure described in the previous section. The dashed curves represent corresponding values from Reference 7, which claims an accuracy of four to five significant digits. The results chosen for presentation here are on purpose not the correct ones; the discrepancies will facilitate the discussion of the computational process.

Figures 2 and 4 together indicate that, as the computation progresses forward, the shock rotates to accomodate to the angle of attack exactly as it did in the unsteady computations reported in Reference 3. The axial distance in which the solution builds up to its correct value is analogous to the time necessary to reach the steady state using the unsteady approach of References 2 and 3. Therefore, in practical applications, Δz must be chosen sufficiently small to allow at least 250 steps between the vertex and the first point at which the solution is desired.

A possible way to circumvent this difficulty is to repeat the computation with the now known surface values at $219\Delta z$ prescribed at the vertex; another alternative will be described in Section VI.

Trial runs on the computer have indicated that in order to stabilize the computations Δz may be only somewhere between 1/2 and 1/3 of the value it is allowed to have by conditions (17) and (18). This is a clear indication of the inadequacy of linear stability theory.

Before closing this discussion it must be pointed out that the leeward surface generator, $\phi=-90°$, is a singular line in the method of Reference 6. Values of all variables at this point, calculated by the method of Reference 6 and tabulated in Reference 7, are obtained by extrapolating both across the shock layer and along the surface and the two extrapolations always yield two distinct values as indicated in Figure 2. The difference between these two values is about the same as the discrepancy between our results and those of Reference 7.

The nonuniqueness of values at the leeward generator in References 6 and 7 is consistent with findings of other investigators who discovered that a singularity occurs there in the linearized treatment of the present problem (e.g., Ferri's vortex singularity). It is therefore fair to conclude that correct values at $\phi=-90°$ cannot be obtained within the framework of inviscid fluid theory.

VI. CONICAL FLOWS

When the body shape beyond the vertex remains a cone with a constant half angle β, then considerable simplification of the boundary logic, economy in memory storage, and avoidance of difficulties associated with the cone vertex are possible with a spherical polar coordinate system shown in Figure 5 where r, for the purposes of this section, denotes distance along the rays.

The form of the equations and their differencing in spherical coordinates are discussed in detail in Reference 3 and need not be reproduced here. The simplification follows from the postulated conical property of the flow which implies that the derivatives of the dependent variables in the radial direction may be discarded leaving only dependence on two angular coordinates. For computational purposes time is introduced as the integration variable and the integration is continued until the steady state is reached, exactly as described in References 2 and 3. In this process the time derivatives appear multiplied by r because the flow is conical only in the steady state limit. However, the stability condition requires that only the ratio $\frac{\Delta t}{r\Delta\theta}$ needs to be specified, hence r does not enter into the problem explicitly.

The more efficient use of core memory is a consequence of the fact that the computing region is similar in shape to the shock layer and therefore it is not necessary to carry many superfluous points of the free stream as in the case of cylindrical coordinates. In addition, since the cone $\theta=\beta$ is now one of the coordinate surfaces, the application of the boundary conditions can be simplified[3] by eliminating the need for an interpolation procedure; this, together with a much finer mesh made possible by the elimination of radial dependence (conical similarity), increases the accuracy of computations.

Results obtained with the above-described computational procedure are presented in Figures 6, 7, and 8. Figure 6 represents the pressure distribution in front of a 35° half angle cone at typical super orbital entry conditions ($M_o \sim 29$, altitude $\sim$ 200,000 ft.) calculated by the present method and compared with more accurate and elaborate computations; the results agree to within a few percent.

Figure 7 represents the complete circumferential surface pressure distribution obtained by the unsteady conical computation for $M_o = 7.95$, $\beta = 10°$, and $\alpha = 20°$. In this figure points indicated by circles are experimental values obtained by Tracy[10]; the agreement appears satisfactory.

In order to further illustrate the extent of the asymmetry of the flow we have prepared Figure 8, which is the view of the surface streamlines from the vertex of the cone. Free stream conditions for this flow pattern are $M_o = 7.95$, $\beta = 10°$, $\alpha = 8°$. The computed flow directions on the surface agree well with the oil slick photographs of models and are useful in calculating the properties in the boundary layer.[11]

VII. CONCLUDING REMARKS

The discussion and results presented in this memorandum indicate that the general approach described in Sections IV, V, and VI produces results which are acceptable for many engineering purposes, is conceptually simple, and is easy to program. The method,therefore, appears sufficiently promising to warrant further development.

The computational procedure described here can be readily improved by, for example, more judicious choice of the mesh (e.g., Reference 12), or by the application of second order accurate differencing schemes that are available (e.g., Reference 13). However, the formulations used in Sections IV and VI possess serious inherent limitations.

The approach presented in Section IV is not uniformly applicable to blunted shapes and it is not suited for the treatment of radiating flows because the computer retains in its memory at one time not the entire field but only two transverse slices of it. It is, however, well suited for the computation of chemically reacting flows and has been used for that purpose successfully by DeJarnette.[12]

The formulation employed in Section VI is valid only for similarity flows, which restricts its applicability to flows over sharp, slender, infinitely long cones at moderate angles of attack. This limitation may be removed by retaining the radial derivatives in the governing system of differential equations. With such generalization, the time-dependent formulation in spherical coordinates remains valid even for cone angles in excess of the critical value at which the bow shock detaches, also for blunted cones, and for flows with mass injection from the solid surface. In addition, the fact that the digital description of the entire flow field is stored in computer memory at all times makes it possible to evaluate the contribution of radiative phenomena. For these reasons this is the approach that we are presently developing at Bellcomm. The difficulties surmounted in the process and the results obtained will be described in a separate document.

Ihor O. Bohachevsky

I. O. Bohachevsky

1034-IOB-bmn

Attachments
References
Appendix
Figures 1-8

REFERENCES

1. Bohachevsky, I. O. and Kostoff, R. N., "Numerical Study of Reentry Phenomena," Bellcomm Memorandum for File, Case 103, October 11, 1968.

2. Bohachevsky, I. O. and Rubin, E. L., "A Direct Method for Computation of Nonequilibrium Flows with Detached Shocks," AIAA Journal, 4, pp. 600-607 (1966).

3. Bohachevsky, I. O. and Mates, R. E., "A Direct Method for Calculation of the Flow about an Axisymmetric Blunt Body at Angle of Attack," AIAA Journal, 4, pp. 776-782 (1966).

4. Ferri, A., "Supersonic Flows with Shock Waves," in "General Theory of High Speed Aerodynamics," W. R. Sears Ed. Vol. VI., pp. 670-747, Princeton University Press, Princeton, New Jersey, 1954.

5. Sedney, R. and Gerber, N., "Nonequilibrium Flow over a Cone," AIAA Journal 1, pp. 2482-2486 (1963).

6. Babenko, K. I. and Voskresenskii, G. P., "Numerical Method for Computation of Three-dimensional, Supersonic External Flow of Gas," Zhur. Vych, Mat. i Mat. Fiziki 1 pp. 1051-1060 (1961).

7. Babenko, K. I., Voskresenskii, G. P., Lubimov, A. N., Rusanov, V. V., "Three-dimensional Flow of an Ideal Gas about Smooth Bodies," Nauka, Moskva 1964 (in Russian).

8. South, J. C. and Newman, P. A., "Application of the Method of Integral Relations to Real Gas Flows Past Pointed Bodies," AIAA Journal 3 pp. 1645-1652 (1965).

9. Belotserkovskii, O. M. Editor: "Flow About Blunt Bodies in a Supersonic Stream of a Gas," Vychislitelnyi Tsentr AN USSR, Moscow (1967).

10. Tracy, R. R., "Hypersonic Flow over a Yawed Circular Cone," GALCIT Memorandum No. 69 (August 1, 1963).

11. Kang, S. W., Rae, W. J., Dunn, M. G., "Effects of Mass Injection on Compressible, Three-dimensional, Laminar Boundary Layers with Small Secondary Flow," Cornell Aeronautical Laboratory, Report No. AI-2187-A-2, Buffalo, New York, August 1966.

12. DeJarnette, F. R.; "Application of Lax's Finite Difference Method to Nonequilibrium Hypersonic Flow Problems," NASA TR R-234, March 1966.

13. Lax, P. and Wendroff, B. "Systems of Conservation Laws," Comm. Pure and Appl. Math., XIII, pp. 217-237 (1960).

APPENDIX

In order to keep the algebra tractable, we restrict ourselves to two independent variables, t and x. The general, homogeneous system of quasilinear partial differential equations for k functions $w = \{w_1, w_2, \ldots w_k\}$ may be written as

$$\frac{\partial w}{\partial t} + T(w)\frac{\partial w}{\partial x} = 0 \tag{A1}$$

where $T = [a_{ij}]$ is a k by k matrix. We wish to introduce new variables $\phi_n(w)$ in such a manner that each ϕ_n will remain constant along some line designated by its slope λ_n, i.e., the relations

$$\frac{\partial \phi_n}{\partial t} + \lambda_n \frac{\partial \phi_n}{\partial x} = 0 \tag{A2}$$

will obtain as a consequence of (A1)

Towards this end we form a linear combination of equations in (A1) with undetermined coefficients μ_i:

$$\sum_{i=1}^{k} \mu_i \frac{\partial w_i}{\partial t} + \sum_{i=1}^{k}\sum_{j=1}^{k} \mu_i a_{ij} \frac{\partial w_j}{\partial x} = 0$$

In the double sum above, we interchange i and j to obtain:

$$\sum_{i=1}^{k} \mu_i \frac{\partial w_i}{\partial t} + \sum_{j=1}^{k}\sum_{i=1}^{k} \mu_j a_{ji} \frac{\partial w_i}{\partial x} = 0 \tag{A3}$$

Now, using the chain rule of differentiation, (A2) becomes:

$$\sum_{i=1}^{k} \frac{\partial \phi_n}{\partial w_i} \frac{\partial w_i}{\partial t} + \lambda_n \sum_{i=1}^{k} \frac{\partial \phi_n}{\partial w_i} \frac{\partial w_i}{\partial x} = 0 \qquad \text{(A4)}$$

Upon comparing (A3) and (A4), we see that μ_i's must satisfy

$$\frac{\partial \phi_n}{\partial w_i} = \mu_i \qquad \text{(A5)}$$

$$\sum_{j=1}^{k} \mu_j \, a_{ji} = \lambda_n \frac{\partial \phi_n}{\partial w_i} = \lambda_n \mu_i \qquad \text{(A6)}$$

A consequence of (A5) is

$$\frac{\partial \mu_i}{\partial w_j} = \frac{\partial \mu_j}{\partial w_i} \qquad \text{(A7)}$$

Thus, for the k functions μ_i, we have derived k equations from (A6) and $\frac{1}{2}$ k (k-1) equations from (A7).

Since k = k + $\frac{1}{2}$ k (k-1) implies k = 1, it may appear that the determination of such ϕ_n is in general not possible. However, for k = 2, (A7) is only one equation which can be satisfied when the μ_i's are multiplied by an integrating factor which always exists by Lie's theory. Therefore, for this case only, the system of equations for μ_i's is not overdetermined.

In gas dynamics ϕ_n's are the Riemann Invariants and λ_n the eigenvalues of T. Therefore, if the flow is isentropic and:

1. one-dimensional unsteady, with variables ρ-density, and u-velocity; or

2. two-dimensional steady, with variables ρ, u, and v (the third partial differential equation in this case is replaced by the Bernuolli's integral)

the Riemann Invariants exist; otherwise, generally not.

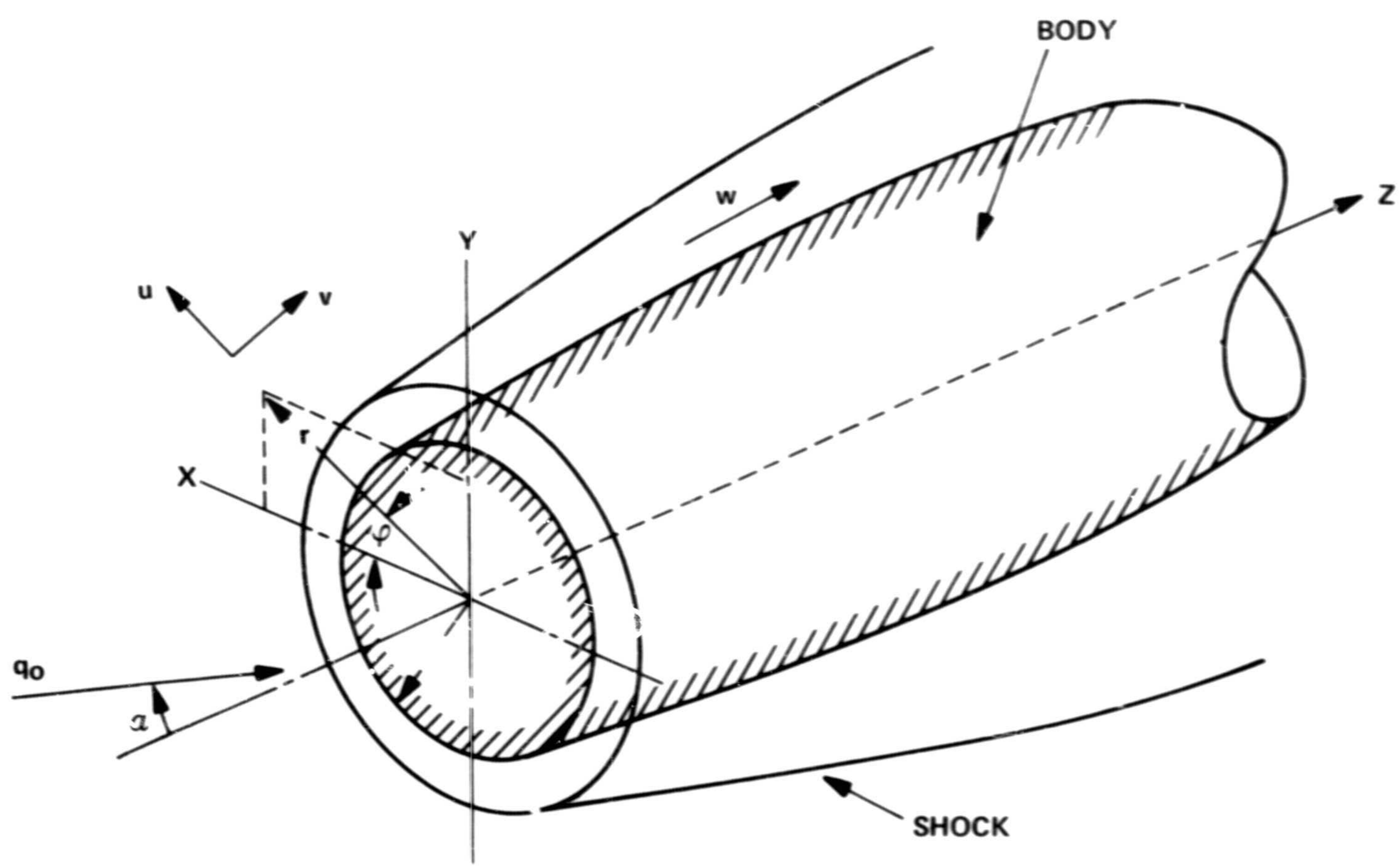

FIGURE 1 - COORDINATE SYSTEM AND SCHEMATIC REPRESENTATION OF FLOW CONFIGURATION

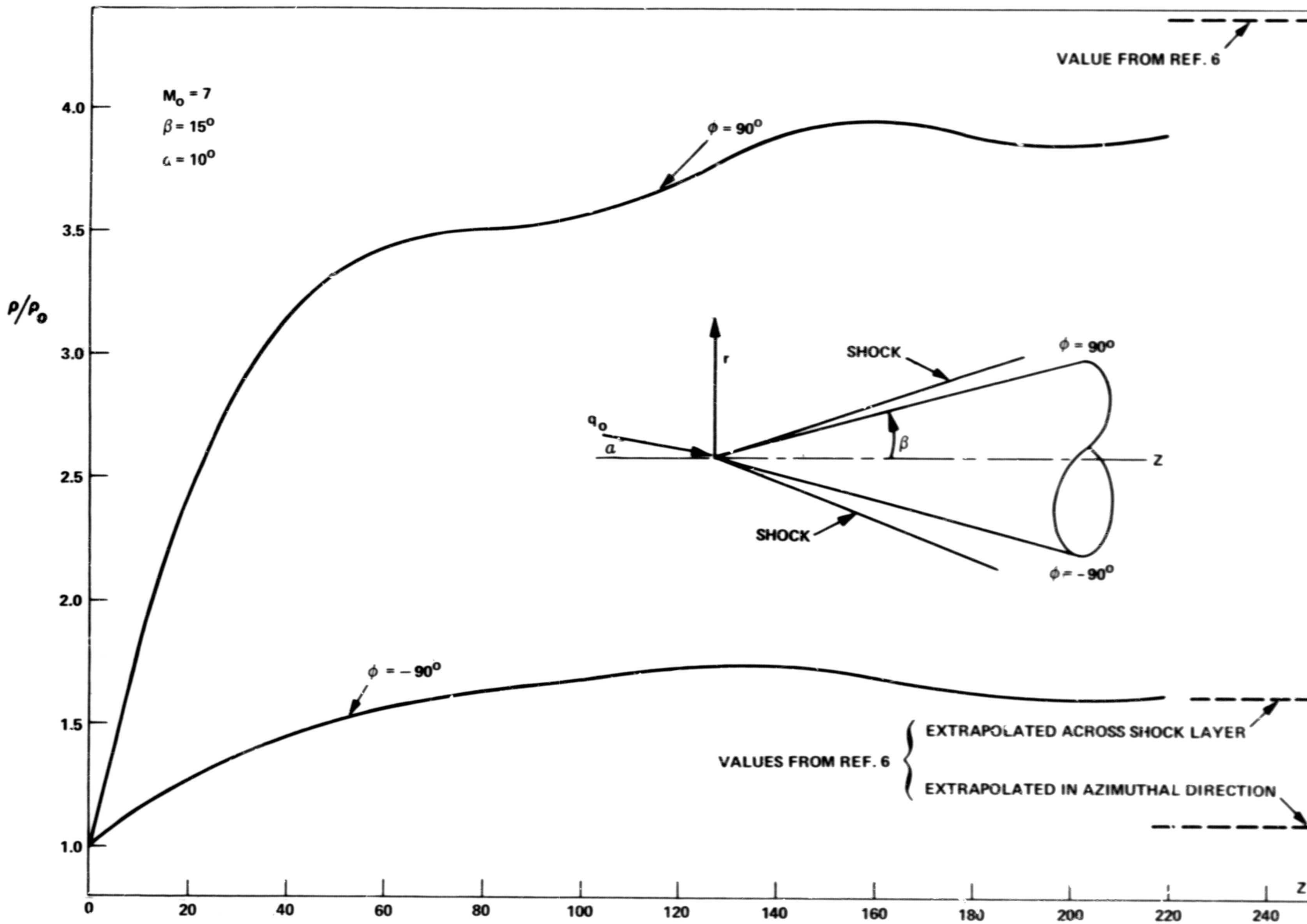

FIGURE 2 - SURFACE DENSITY DISTRIBUTION

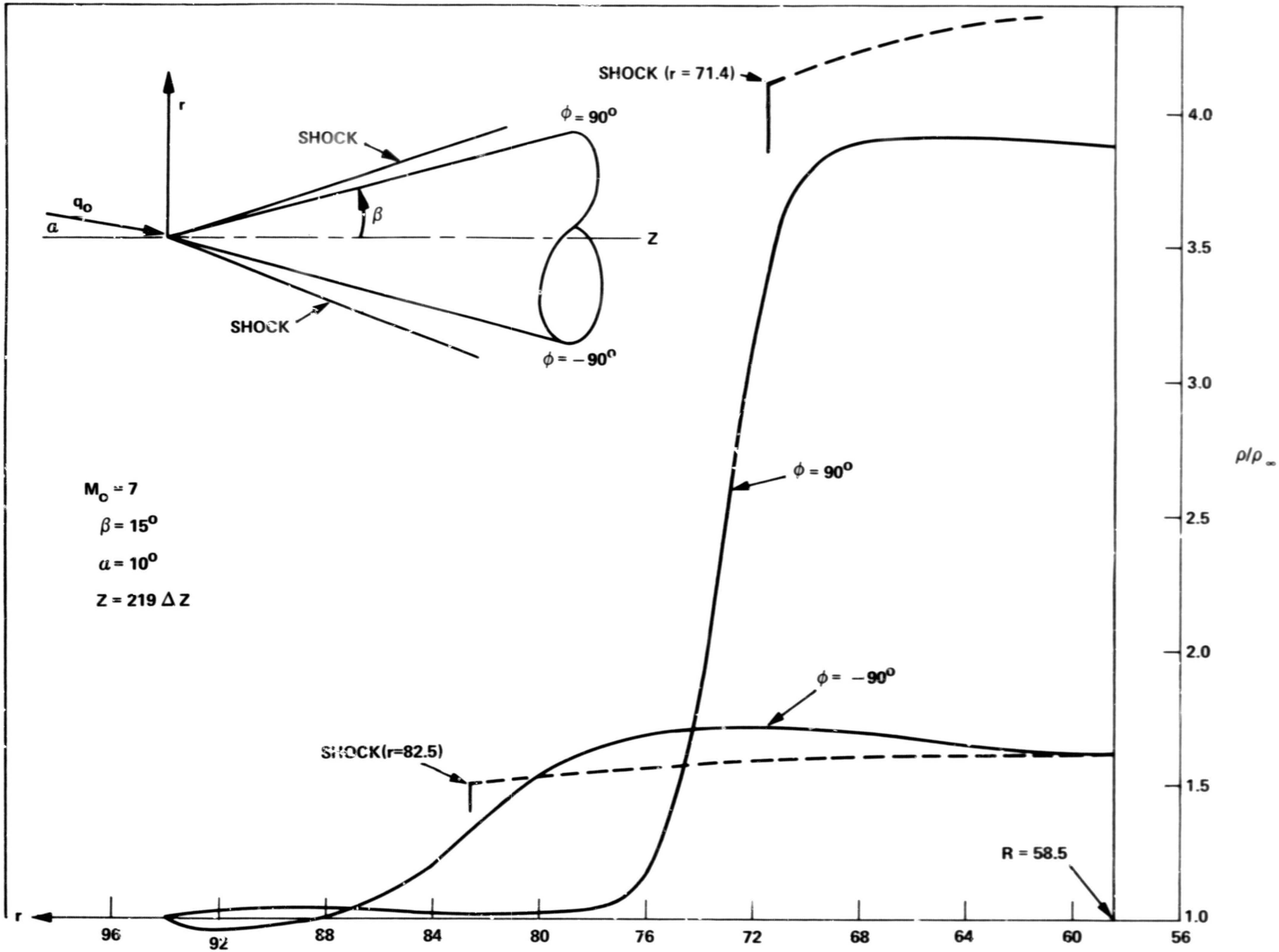

FIGURE 3 - DENSITY DISTRIBUTION

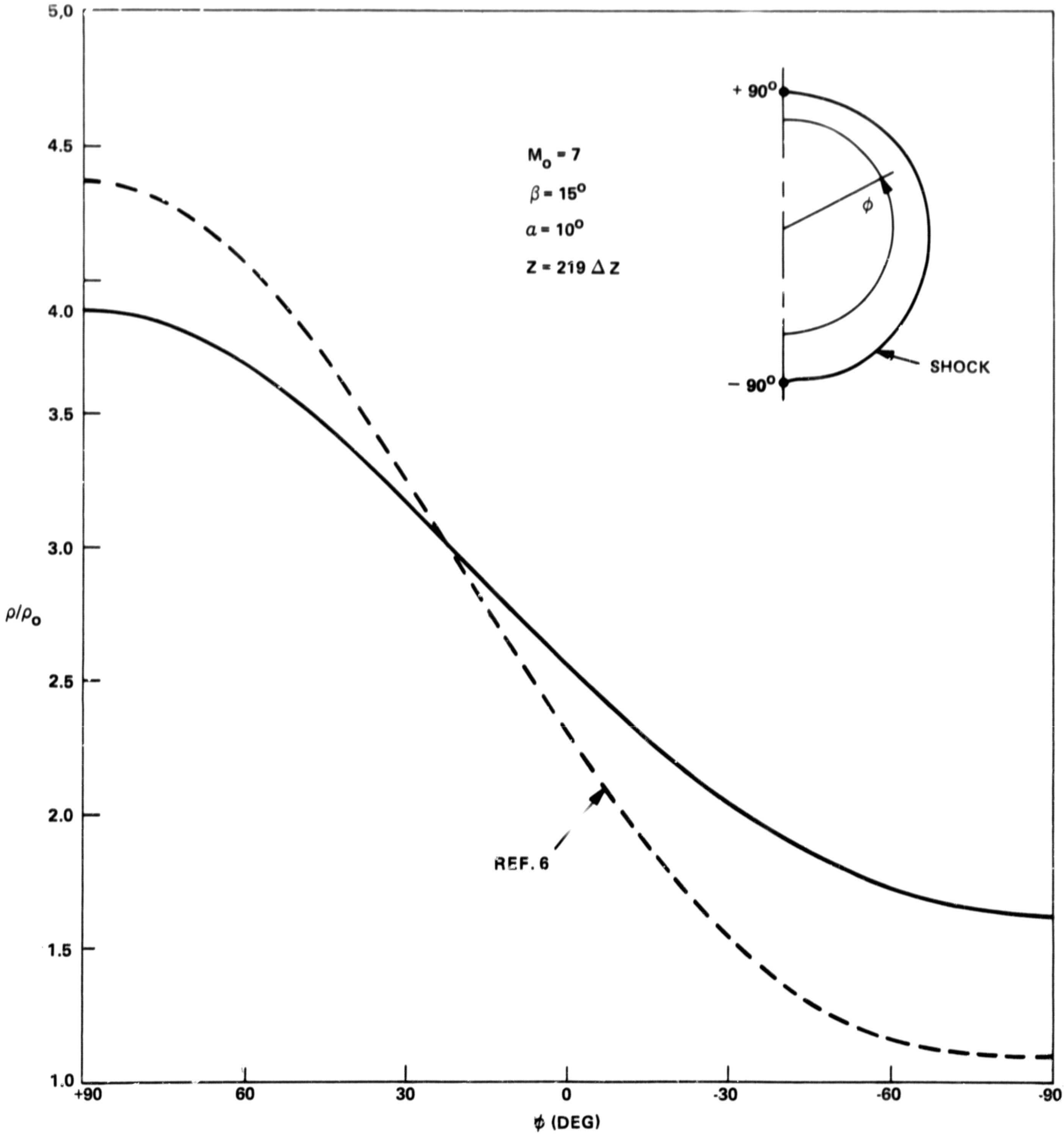

FIGURE 4 - AZIMUTHAL SURFACE DENSITY DISTRIBUTION

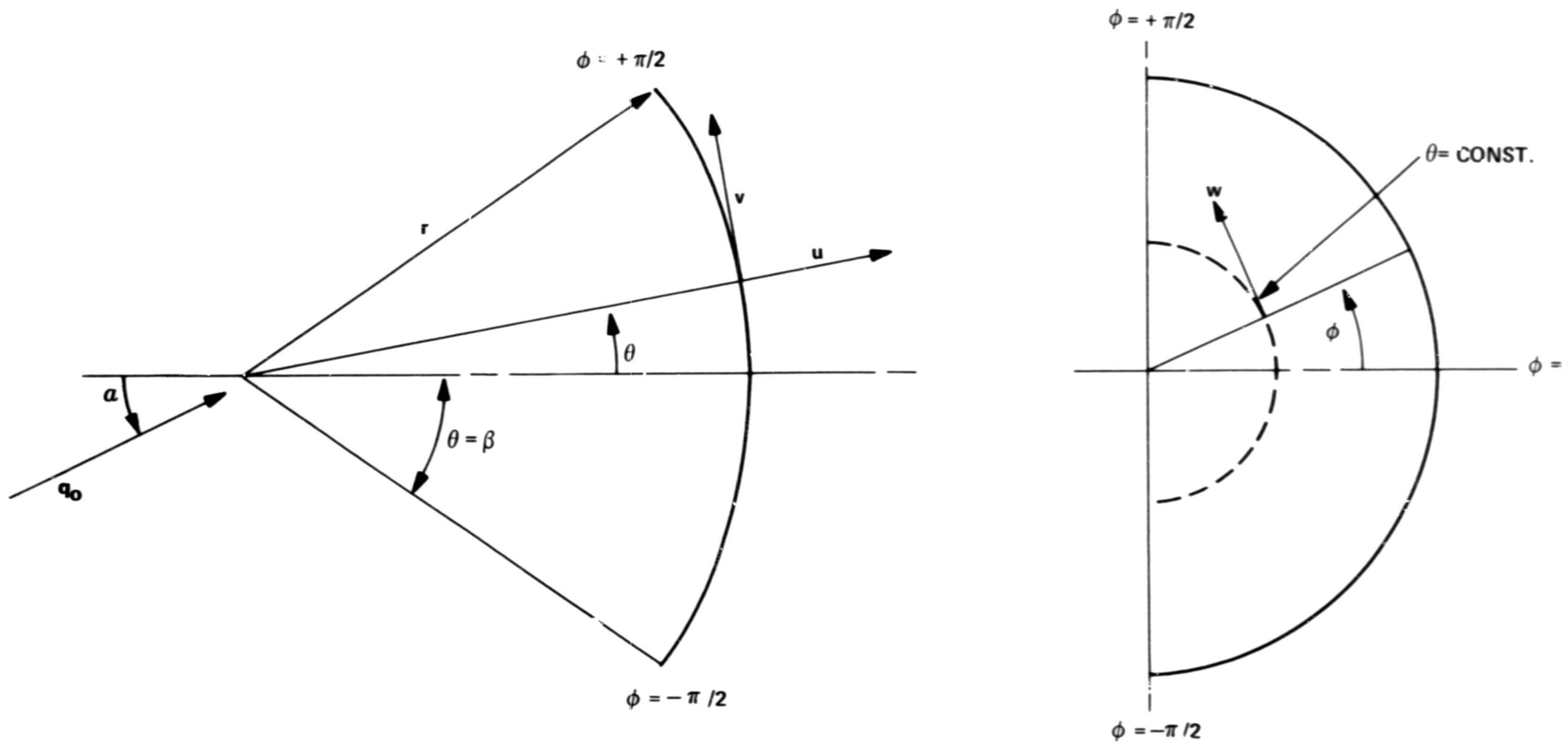

FIGURE 5 - SPHERICAL COORDINATE SYSTEM

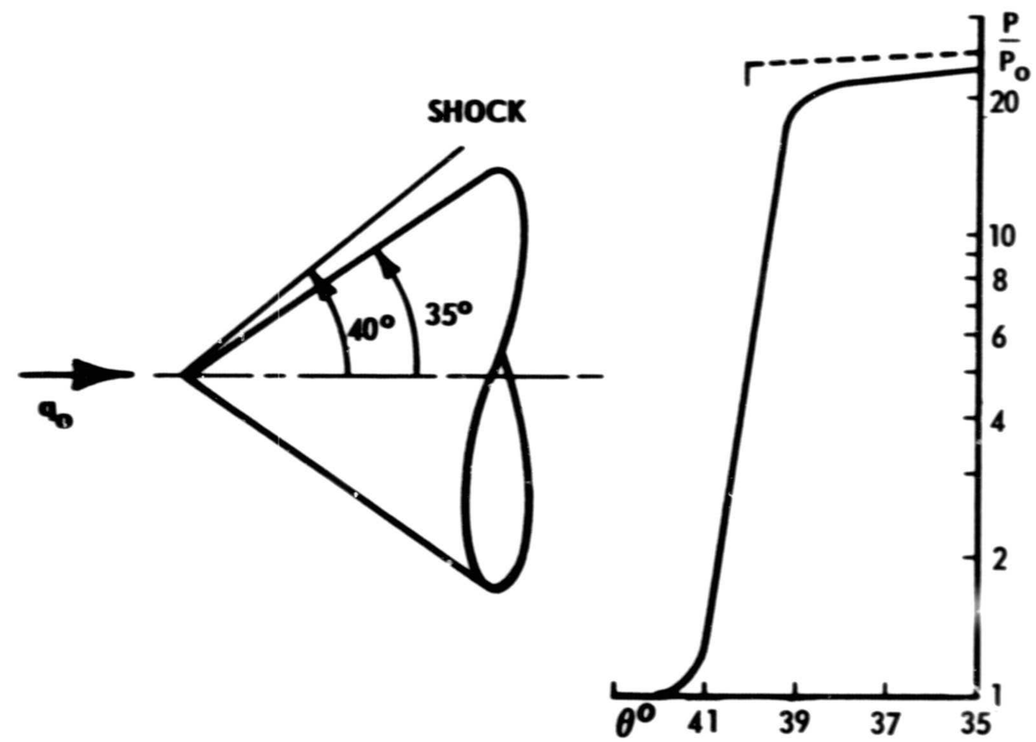

FIGURE 6 - NORMAL PRESSURE DISTRIBUTION

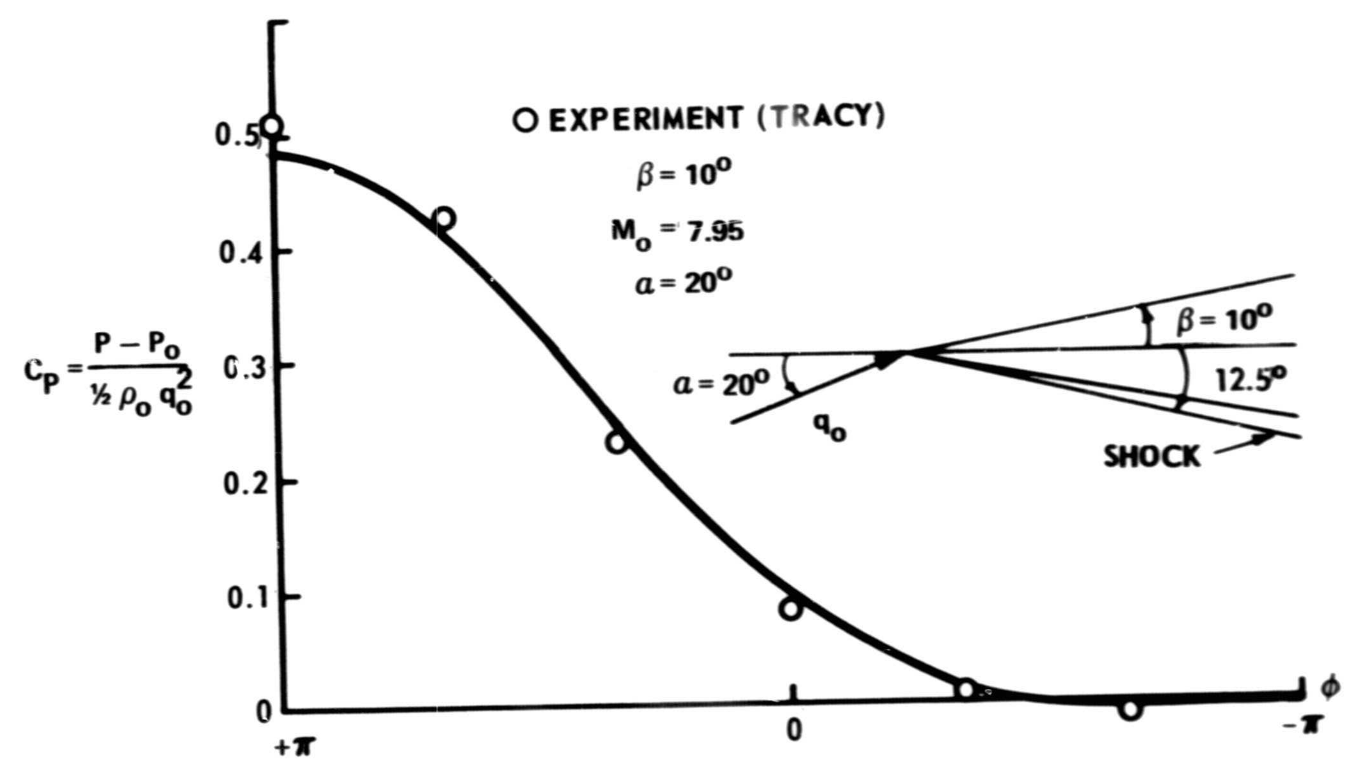

FIGURE 7 - CIRCUMFERENTIAL PRESSURE DISTRIBUTION

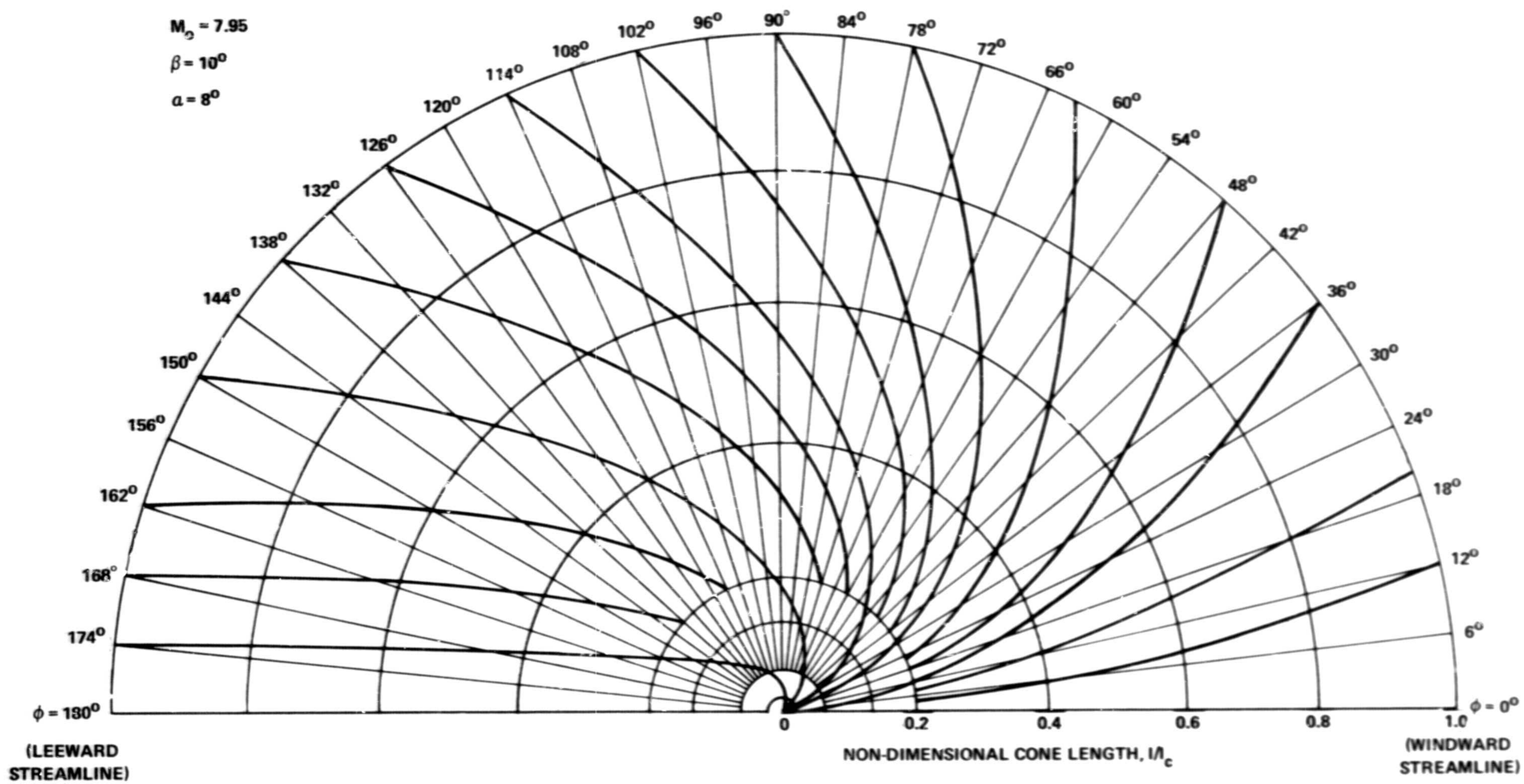

FIGURE 8 - STREAMLINE PATTERN